Journal of Zhejiang University-SCIENCE A (Applied Physics & Engineering)
ISSN 1673-565X (Print); ISSN 1862-1775 (Online)
www.zju.edu.cn/jzus; www.springerlink.com
E-mail: jzus@zju.edu.cn

Propagation of flexural waves in phononic crystal thin plates with linear defects*

Zong-jian YAO†, Gui-lan YU†‡, Yue-sheng WANG, Zhi-fei SHI, Jian-bao LI

(*School of Civil Engineering, Beijing Jiaotong University, Beijing 100044, China*)

†E-mail: 04121142@bjtu.edu.cn; glyu@bjtu.edu.cn

Received Mar. 28, 2010; Revision accepted May 25, 2010; Crosschecked Sept. 13, 2010

Abstract: The band structures of flexural waves in a phononic crystal thin plate with straight, bending or branching linear defects are theoretically investigated using the supercell technique based on the improved plane wave expansion method. We show the existence of an absolute band gap of the perfect phononic crystal and linear defect modes inside the gap caused by localization of flexural waves at or near the defects. The displacement distributions show that flexural waves can transmit well along the straight linear defect created by removing one row of cylinders from the perfect phononic crystals for almost all the frequencies falling in the band gap, which indicates that this structure can act as a high efficiency waveguide. However, for bending or branching linear defects, there exist both guided and localized modes, and therefore the phononic crystals could be served as waveguides or filters.

Key words: Phononic crystal, Thin plates, Linear defects, Flexural waves
doi:10.1631/jzus.A1000123 **Document code:** A **CLC number:** O322

1 Introduction

In the past few years, the propagation of elastic waves in acoustic band gap materials, known as phononic crystals, has attracted much attention. One important feature of phononic crystals is the existence of the absolute phononic band gaps, in which elastic waves cannot propagate. This has encouraged many researchers to study on the band gap characteristics of perfect bulk phononic crystals (Tanaka and Tamura, 1998; Bria and Djafari-Rouhani, 2002; Wu T.T. *et al.*, 2004; Yan and Wang, 2006; Yan *et al.*, 2008; Zhang *et al.*, 2010) and perfect phononic crystal plates (Sigalas and Economou, 1994; Hsu and Wu, 2006; Yu *et al.*, 2006). Bulk waves propagating in the phononic crystals with point defects or linear defects have been further studied through extensive theoretical and experimental investigation. Existence of the localized and guided modes inside the band gaps makes it possible for the phononic crystals with point or linear defects to serve as novel microcavities (Khelif *et al.*, 2003a; Wu F.G. *et al.*, 2004; Zhong *et al.*, 2005), high efficiency waveguides (Sigalas, 1998; Kafesaki *et al.*, 2001; Khelif *et al.*, 2004; Zhang *et al.*, 2004; Yao *et al*., 2007), frequency demultipliers (Khelif *et al.*, 2003b; Pennec *et al.*, 2004; Benchabane *et al.*, 2005), and frequency couplers (Li and Liu, 2005; Sun and Wu, 2005), etc.

Some studies have also been conducted for phononic crystal plates with defects. For example, Charles *et al*. (2006) calculated the dispersion relations of guided waves in two different kinds of 2D phononic crystal plates using the plane wave expansion method. Sun and Wu (2007) studied the Lamb wave propagation in a phononic crystal plate and related linear defects using the finite-difference time-domain (FDTD) method. Vasseur *et al*. (2007) investigated the possible practical application of linear defect modes based on a piezoelectric phononic crystal plate freestanding or deposited on a silicon substrate using the finite element method (FEM). Also, using the FDTD method and the FEM,

‡ Corresponding author

* Project (Nos. 10632020 and 90715006) supported by the National Natural Science Foundation of China

Pennec *et al*. (2008) investigated the band structures of Lamb waves in a phononic crystal consisting of cylindrical dots deposited on a thin plate, and the propagation of Lamb waves in the linear defect was also studied. It is worth mentioning that based on the general 3D theory, Vasseur *et al*. (2008) have studied the propagation of Lamb waves in a plate. In the solid-solid systems, the calculations of the band structures suffered from the convergence problem because of the limited number of reciprocal vectors. In the case of air-solid systems, they found that the existence of absolute band gaps occur in the band structures provided that the thickness of the plate is in the order of the lattice parameter.

It is known that the flexural waves are mainly concerned when the plate thickness is relatively small (Sigalas and Economou, 1994; Yu *et al.*, 2006). As yet there is no literature devoted to the investigations of flexural waves in phononic crystal plates with defects except that of the present authors (Yao *et al.*, 2009) who investigated the propagation of flexural waves in a phononic crystal thin plate with a point defect based on the classical plate theory.

Here, we extend our investigations to the case of linear defects. The aim of this paper is to calculate the dispersion relations for the phononic crystal thin plate with straight, bending or branching linear defects respectively, and to present the displacement distributions associated with the linear defect modes. The improved plane wave expansion method combined with the supercell technique is employed for the analysis. Obviously, the work presented in this paper is subsequent to Yao *et al.* (2009).

2 Methods

The perfect phononic crystal thin plate shown in Fig. 1a is composed of an infinite periodic square array of cylinders (material A) embedded in a host matrix (material B). A simple straight linear defect, which is constructed by removing a period row of cylinders along (1,0) direction from the perfect structure, is depicted in Fig. 1b. A bending linear defect could be constructed by removing cylinders in (1,0)/(1,1) direction shown in Fig. 1c. Fig. 1d shows the *x*-axis symmetrical branching linear defect along (1,0)/(1,1)/(1,−1) direction. The thickness of the thin plate, the lattice constant, and the radius of the inclusive cylinder are denoted by h, a, and r_0, respectively, which are shown in a unit cell (Fig. 1e).

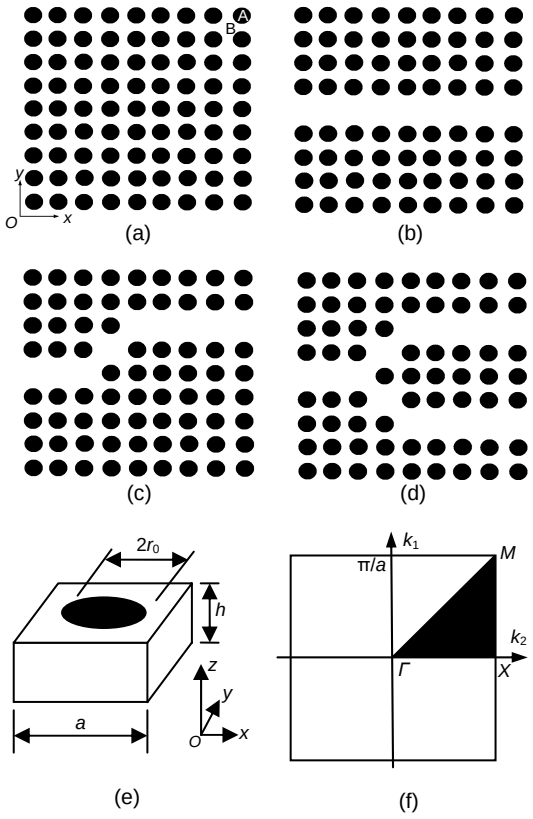

Fig. 1 Top views of the infinite phononic crystal thin plate

(a) Perfect structure; (b) Straight linear defect; (c) Bending linear defect; (d) Branching linear defect; (e) Unit cell; (f) The first Brilloun zone of the unit cell, and the triangle $\Delta\Gamma XM$ represents the first irreducible Brilloun zone

In terms of the (x,y,z)-coordinate system, where x- and y-axes are in the plane of the plate as shown in Fig. 1a, the equation governing the bending of a plate with uniform thickness is (Sigalas and Economou, 1994; Yao *et al.*, 2009)

$$-\alpha\frac{\partial^2 w}{\partial t^2}=\frac{\partial^2}{\partial x^2}\left(D\frac{\partial^2 w}{\partial x^2}+\beta\frac{\partial^2 w}{\partial y^2}\right)+2\frac{\partial^2}{\partial x\partial y}\left(\gamma\frac{\partial^2 w}{\partial x\partial y}\right)+\frac{\partial^2}{\partial y^2}\left(D\frac{\partial^2 w}{\partial y^2}+\beta\frac{\partial^2 w}{\partial x^2}\right), \tag{1}$$

where w is the transverse displacement in the z-direction; $D=Eh^3/(12(1-\upsilon^2))$ is the flexural rigidity with E being the Young's modulus and υ the

Poisson's ratio; $\alpha=\rho h$, $\beta=D\upsilon$, and $\gamma=D(1-\upsilon)$. All of these variables are periodic functions of the position vector $\boldsymbol{r}=(x, y)$.

According to Bloch's theorem, the displacement field of harmonic waves in the phononic crystal thin plate can be expressed as

$$\boldsymbol{w}(\boldsymbol{r},t)=\mathrm{e}^{i(\boldsymbol{k}\boldsymbol{r}-\omega t)}w_{\boldsymbol{k}}(\boldsymbol{r}), \tag{2}$$

where $\boldsymbol{k}=(k_1,k_2)$ is the Bloch wave vector and ω the angular frequency; $w_{\boldsymbol{k}}(\boldsymbol{r})$ is a periodic function with the same spatial periodicity as the structure and can be expanded in Fourier series as

$$w_{\boldsymbol{k}}(\boldsymbol{r})=\sum_{\boldsymbol{G}_1}\mathrm{e}^{i\boldsymbol{G}_1\boldsymbol{r}}A_{\boldsymbol{G}_1}, \tag{3}$$

where $\boldsymbol{G}_1=2\pi(n_1/a, n_2/a)$ is the 2D reciprocal lattice vector with n_1, $n_2=0, \pm1, \pm2, \ldots, \pm n$, and $A_{\boldsymbol{G}_1}$ is the corresponding Fourier coefficient.

According to the conventional plane wave expansion method, all material parameters should be directly expanded in Fourier series according to the spatial periodicity. However, in the improved plane wave expansion method, all the inversed material parameters are expanded in Fourier series in order to obtain a good convergence (Li, 1996; Cao *et al.*, 2004). For the present problem, we expand $1/\alpha(\boldsymbol{r})$, $1/\beta(\boldsymbol{r})$, $1/D(\boldsymbol{r})$, and $1/\gamma(\boldsymbol{r})$ in Fourier series of the following form (Yao *et al.*, 2009):

$$H(\boldsymbol{r})=\sum_{\boldsymbol{G}_2}\mathrm{e}^{i\boldsymbol{G}_2\boldsymbol{r}}H_{\boldsymbol{G}_2}, \tag{4}$$

where $H(\boldsymbol{r})$ can be one of $1/\alpha(\boldsymbol{r})$, $1/\beta(\boldsymbol{r})$, $1/D(\boldsymbol{r})$ or $1/\gamma(\boldsymbol{r})$; $H_{\boldsymbol{G}_2}$ is the corresponding Fourier coefficient. To keep the neighboring linear defects far from each other, a 9×9 supercell is chosen here to avoid the interaction between the simulated linear defects, and then we have the Fourier coefficient in Eq. (5.1) for the straight linear defect, Eq. (5.2) for the bending linear defect, and Eq. (5.3) for for the branching linear defect, where $\boldsymbol{G}_2=2\pi(n_1/9a, n_2/9a)$ is the reciprocal lattice vector with n_1, $n_2=0, \pm1, \pm2, \ldots, \pm n$, $f=\pi r_0^2/a^2$, $F_{\boldsymbol{G}_2}=2fJ_1(|\boldsymbol{G}_2|r_0)/(|\boldsymbol{G}_2|r_0)$, $J_1(|\boldsymbol{G}_2|r_0)$ and $f_\mathrm{d}=\pi r_\mathrm{d}^2/a^2$, $F_{\boldsymbol{G}_2}^\mathrm{d}=2f_\mathrm{d}J_1(|\boldsymbol{G}_2|r_\mathrm{d})/(|\boldsymbol{G}_2|r_\mathrm{d})$, $J_1(|\boldsymbol{G}_2|r_\mathrm{d})$ are the filling fraction, structure function, and the first kind Bessel function of the first order corresponding to the perfect cylinder and the defect cylinder, respectively (where r_d is the radius of the defect cylinders, here $r_\mathrm{d}=0$).

Substitute Eqs. (2)–(5) into Eq. (1), we have the following eigen-value problem

$$\begin{aligned}
\omega^2\sum_{\boldsymbol{G}_1}[\![\boldsymbol{\alpha}]\!]_{\boldsymbol{G}_2}^{-1}\boldsymbol{A}_{\boldsymbol{k}+\boldsymbol{G}_1}&=\sum_{\boldsymbol{G}_1}(\boldsymbol{k}+\boldsymbol{G}_1)_x^2(\boldsymbol{k}+\boldsymbol{G}_3)_x^2[\![1/\boldsymbol{D}]\!]_{\boldsymbol{G}_2}^{-1}\boldsymbol{A}_{\boldsymbol{k}+\boldsymbol{G}_1}\\
&+\sum_{\boldsymbol{G}_1}(\boldsymbol{k}+\boldsymbol{G}_1)_y^2(\boldsymbol{k}+\boldsymbol{G}_3)_x^2[\![1/\boldsymbol{\beta}]\!]_{\boldsymbol{G}_2}^{-1}\boldsymbol{A}_{\boldsymbol{k}+\boldsymbol{G}_1}\\
&+2\sum_{\boldsymbol{G}_1}(\boldsymbol{k}+\boldsymbol{G}_1)_x(\boldsymbol{k}+\boldsymbol{G}_1)_y(\boldsymbol{k}+\boldsymbol{G}_3)_x(\boldsymbol{k}+\boldsymbol{G}_3)_y[\![1/\boldsymbol{\gamma}]\!]_{\boldsymbol{G}_2}^{-1}\boldsymbol{A}_{\boldsymbol{k}+\boldsymbol{G}_1}\\
&+\sum_{\boldsymbol{G}_1}(\boldsymbol{k}+\boldsymbol{G}_1)_y^2(\boldsymbol{k}+\boldsymbol{G}_3)_y^2[\![1/\boldsymbol{D}]\!]_{\boldsymbol{G}_2}^{-1}\boldsymbol{A}_{\boldsymbol{k}+\boldsymbol{G}_1}\\
&+\sum_{\boldsymbol{G}_1}(\boldsymbol{k}+\boldsymbol{G}_1)_x^2(\boldsymbol{k}+\boldsymbol{G}_3)_y^2[\![1/\boldsymbol{\beta}]\!]_{\boldsymbol{G}_2}^{-1}\boldsymbol{A}_{\boldsymbol{k}+\boldsymbol{G}_1},
\end{aligned} \tag{6}$$

where $\boldsymbol{G}_3=\boldsymbol{G}_1+\boldsymbol{G}_2$ and $[\![\boldsymbol{H}]\!]_{\boldsymbol{G}_2}^{-1}$ denotes the inverse of the toeplitz matrix $[\![\boldsymbol{H}]\!]_{\boldsymbol{G}_2}$ with elements shown in Eqs. (5.1)–(5.3) for different kinds of the linear defect. Truncating the series in Eq. (6) to finite sums consisting of N terms, we can obtain $N\times N$ equations, and Eq. (6) can then be rewritten in the matrix form

$$\omega^2\boldsymbol{P}\boldsymbol{A}_{\boldsymbol{k}+\boldsymbol{G}_1}=\boldsymbol{Q}\boldsymbol{A}_{\boldsymbol{k}+\boldsymbol{G}_1}, \tag{7}$$

where $\boldsymbol{P}$ and $\boldsymbol{Q}$ are $N\times N$ matrixes,

$$\boldsymbol{P}=\sum_{\boldsymbol{G}_1}[\![\boldsymbol{\alpha}]\!]_{\boldsymbol{G}_2}, \tag{8}$$

$$\begin{aligned}
\boldsymbol{Q}&=\sum_{\boldsymbol{G}_1}(\boldsymbol{k}+\boldsymbol{G}_1)_x^2(\boldsymbol{k}+\boldsymbol{G}_3)_x^2[\![1/\boldsymbol{D}]\!]_{\boldsymbol{G}_2}^{-1}\\
&+\sum_{\boldsymbol{G}_1}(\boldsymbol{k}+\boldsymbol{G}_1)_y^2(\boldsymbol{k}+\boldsymbol{G}_3)_x^2[\![1/\boldsymbol{\beta}]\!]_{\boldsymbol{G}_2}^{-1}\\
&+2\sum_{\boldsymbol{G}_1}(\boldsymbol{k}+\boldsymbol{G}_1)_x(\boldsymbol{k}+\boldsymbol{G}_1)_y(\boldsymbol{k}+\boldsymbol{G}_3)_x(\boldsymbol{k}+\boldsymbol{G}_3)_y[\![1/\boldsymbol{\gamma}]\!]_{\boldsymbol{G}_2}^{-1}\\
&+\sum_{\boldsymbol{G}_1}(\boldsymbol{k}+\boldsymbol{G}_1)_y^2(\boldsymbol{k}+\boldsymbol{G}_3)_y^2[\![1/\boldsymbol{D}]\!]_{\boldsymbol{G}_2}^{-1}\\
&+\sum_{\boldsymbol{G}_1}(\boldsymbol{k}+\boldsymbol{G}_1)_x^2(\boldsymbol{k}+\boldsymbol{G}_3)_y^2[\![1/\boldsymbol{\beta}]\!]_{\boldsymbol{G}_2}^{-1}.
\end{aligned} \tag{9}$$

By solving Eq. (7) for the specific Bloch wave vector $\boldsymbol{k}$, the eigen-frequency ω can be obtained which yields the band structures.

$$
H_{\boldsymbol{G}_2}=\begin{cases}
\dfrac{1}{81}\left\{72\left[fH_{\mathrm{A}}+(1-f)H_{\mathrm{B}}\right]+9f_{\mathrm{d}}H_{\mathrm{A}}+9(1-f_{\mathrm{d}})H_{\mathrm{B}}\right\}, \text{ for } \boldsymbol{G}_2=0,\\
\dfrac{1}{81}(H_{\mathrm{A}}-H_{\mathrm{B}})\left\{\left[\sum_{m_1=-4}^{4}\sum_{m_2=-4}^{4}\cos\left(\dfrac{2\pi}{9}(m_1n_1+m_2n_2)\right)-\cos\left(-\dfrac{8\pi}{9}n_1\right)-\cos\left(-\dfrac{6\pi}{9}n_1\right)-\cos\left(-\dfrac{4\pi}{9}n_1\right)\right.\right.\\
\qquad -\cos\left(-\dfrac{2\pi}{9}n_1\right)-1-\cos\left(\dfrac{2\pi}{9}n_1\right)-\cos\left(\dfrac{4\pi}{9}n_1\right)-\cos\left(\dfrac{6\pi}{9}n_1\right)-\cos\left(\dfrac{8\pi}{9}n_1\right)\Big]F_{\boldsymbol{G}_2}\\
\qquad -\Big[\cos\left(-\dfrac{8\pi}{9}n_1\right)+\cos\left(-\dfrac{6\pi}{9}n_1\right)+\cos\left(-\dfrac{4\pi}{9}n_1\right)+\cos\left(-\dfrac{2\pi}{9}n_1\right)+1+\cos\left(\dfrac{2\pi}{9}n_1\right)\\
\qquad \left.+\cos\left(\dfrac{4\pi}{9}n_1\right)+\cos\left(\dfrac{6\pi}{9}n_1\right)+\cos\left(\dfrac{8\pi}{9}n_1\right)\Big]F^{\mathrm{d}}_{\boldsymbol{G}_2}\right\}, \text{ for } \boldsymbol{G}_2\neq 0,
\end{cases}
\tag{5.1}
$$

$$
H_{\boldsymbol{G}_2}=\begin{cases}
\dfrac{1}{81}\left\{72\left[fH_{\mathrm{A}}+(1-f)H_{\mathrm{B}}\right]+9f_{\mathrm{d}}H_{\mathrm{A}}+9(1-f_{\mathrm{d}})H_{\mathrm{B}}\right\}, \text{ for } \boldsymbol{G}_2=0,\\
\dfrac{1}{81}(H_{\mathrm{A}}-H_{\mathrm{B}})\left\{\left[\sum_{m_1=-4}^{4}\sum_{m_2=-4}^{4}\cos\left(\dfrac{2\pi}{9}(m_1n_1+m_2n_2)\right)-\cos\left(-\dfrac{8\pi}{9}n_1\right)-\cos\left(-\dfrac{6\pi}{9}n_1\right)-\cos\left(-\dfrac{4\pi}{9}n_1\right)\right.\right.\\
\qquad -\cos\left(-\dfrac{2\pi}{9}n_1+\dfrac{2\pi}{9}n_2\right)-\cos\left(\dfrac{4\pi}{9}n_2\right)-\cos\left(\dfrac{2\pi}{9}n_1+\dfrac{4\pi}{9}n_2\right)-\cos\left(\dfrac{4\pi}{9}n_1+\dfrac{4\pi}{9}n_2\right)\\
\qquad \left.-\cos\left(\dfrac{6\pi}{9}n_1+\dfrac{4\pi}{9}n_2\right)-\cos\left(\dfrac{8\pi}{9}n_1+\dfrac{4\pi}{9}n_2\right)\Big]F_{\boldsymbol{G}_2}+\Big[\cos\left(-\dfrac{8\pi}{9}n_1\right)+\cos\left(-\dfrac{6\pi}{9}n_1\right)\right.\\
\qquad +\cos\left(-\dfrac{4\pi}{9}n_1\right)+\cos\left(-\dfrac{2\pi}{9}n_1+\dfrac{2\pi}{9}n_2\right)+\cos\left(\dfrac{4\pi}{9}n_2\right)+\cos\left(\dfrac{2\pi}{9}n_1+\dfrac{4\pi}{9}n_2\right)\\
\qquad \left.\left.+\cos\left(\dfrac{4\pi}{9}n_1+\dfrac{4\pi}{9}n_2\right)+\cos\left(\dfrac{6\pi}{9}n_1+\dfrac{4\pi}{9}n_2\right)+\cos\left(\dfrac{8\pi}{9}n_1+\dfrac{4\pi}{9}n_2\right)\Big]F^{\mathrm{d}}_{\boldsymbol{G}_2}\right\}, \text{ for } \boldsymbol{G}_2\neq 0,
\end{cases}
\tag{5.2}
$$

$$
H_{\boldsymbol{G}_2}=\begin{cases}
\dfrac{1}{81}\left\{66\left[fH_{\mathrm{A}}+(1-f)H_{\mathrm{B}}\right]+15f_{\mathrm{d}}H_{\mathrm{A}}+15(1-f_{\mathrm{d}})H_{\mathrm{B}}\right\}, \text{ for } \boldsymbol{G}_2=0,\\
\dfrac{1}{81}(H_{\mathrm{A}}-H_{\mathrm{B}})\left\{\left[\sum_{m_1=-4}^{4}\sum_{m_2=-4}^{4}\cos\left(\dfrac{2\pi}{9}(m_1n_1+m_2n_2)\right)-\cos\left(-\dfrac{8\pi}{9}n_1\right)-\cos\left(-\dfrac{6\pi}{9}n_1\right)-\cos\left(-\dfrac{4\pi}{9}n_1\right)\right.\right.\\
\quad -\cos\left(-\dfrac{2\pi}{9}n_1+\dfrac{2\pi}{9}n_2\right)-\cos\left(\dfrac{4\pi}{9}n_2\right)-\cos\left(\dfrac{2\pi}{9}n_1+\dfrac{4\pi}{9}n_2\right)-\cos\left(\dfrac{4\pi}{9}n_1+\dfrac{4\pi}{9}n_2\right)\\
\quad -\cos\left(\dfrac{6\pi}{9}n_1+\dfrac{4\pi}{9}n_2\right)-\cos\left(\dfrac{8\pi}{9}n_1+\dfrac{4\pi}{9}n_2\right)-\cos\left(-\dfrac{2\pi}{9}n_1-\dfrac{2\pi}{9}n_2\right)-\cos\left(-\dfrac{4\pi}{9}n_2\right)\\
\quad -\cos\left(-\dfrac{2\pi}{9}n_1+\dfrac{4\pi}{9}n_2\right)-\cos\left(-\dfrac{4\pi}{9}n_1+\dfrac{4\pi}{9}n_2\right)+\cos\left(-\dfrac{6\pi}{9}n_1+\dfrac{4\pi}{9}n_2\right)+\cos\left(-\dfrac{8\pi}{9}n_1+\dfrac{4\pi}{9}n_2\right)\Big]F_{\boldsymbol{G}_2}\\
\quad +\Big[\cos\left(-\dfrac{8\pi}{9}n_1\right)+\cos\left(-\dfrac{6\pi}{9}n_1\right)+\cos\left(-\dfrac{4\pi}{9}n_1\right)+\cos\left(-\dfrac{2\pi}{9}n_1+\dfrac{2\pi}{9}n_2\right)+\cos\left(\dfrac{4\pi}{9}n_2\right)\\
\quad +\cos\left(\dfrac{2\pi}{9}n_1+\dfrac{4\pi}{9}n_2\right)+\cos\left(\dfrac{4\pi}{9}n_1+\dfrac{4\pi}{9}n_2\right)+\cos\left(\dfrac{6\pi}{9}n_1+\dfrac{4\pi}{9}n_2\right)+\cos\left(\dfrac{8\pi}{9}n_1+\dfrac{4\pi}{9}n_2\right)\\
\quad +\cos\left(-\dfrac{2\pi}{9}n_1-\dfrac{2\pi}{9}n_2\right)+\cos\left(-\dfrac{4\pi}{9}n_2\right)+\cos\left(-\dfrac{2\pi}{9}n_1+\dfrac{4\pi}{9}n_2\right)+\cos\left(-\dfrac{4\pi}{9}n_1+\dfrac{4\pi}{9}n_2\right)\\
\quad \left.\left.+\cos\left(-\dfrac{6\pi}{9}n_1+\dfrac{4\pi}{9}n_2\right)+\cos\left(-\dfrac{8\pi}{9}n_1+\dfrac{4\pi}{9}n_2\right)\Big]F^{\mathrm{d}}_{\boldsymbol{G}_2}\right\}, \text{ for } \boldsymbol{G}_2\neq 0.
\end{cases}
\tag{5.3}
$$

Noted that the classical plate theory used in this study is applicable only for a thin plate and long wavelengths, that is $kh \ll 1$ and $h/a \ll 1$. Mindlin's plate theory could avoid this limitation, but it is more complex mathematically (Hsu and Wu, 2006).

3 Results and discussion

We particular consider the phononic crystal thin plate formed by a square array of Al_2O_3 cylinders embedded in an epoxy matrix. The elastic properties of each constitutive material used in the calculations are the mass density ρ, the Young's modulus E, and the Poisson's ratio υ. For Al_2O_3, ρ_A=3970 kg/m^3, E_A=402.7 GPa, and υ_A=0.23; for epoxy, ρ_B=1142 kg/m^3, E_B=4.35 GPa, and υ_B=0.37. The thickness of the plate is h=0.1a, and the transverse wave velocity in epoxy is C_t=1160 m/s. The filling fraction is $f=\pi r_0^2/a^2$=0.283. In the calculations, 57×57 (n=28) reciprocal vectors per supercell are used in the expanding periodic functions and the convergence is satisfactory. The band structures of the perfect phononic crystal thin plate are shown in part A, Fig. 2, and one can see that there is a wide band gap ranging from 3.32 to 4.45.

3.1 Straight linear defect

First, we consider the properties of the phononic crystal thin plate containing a simple straight linear defect constructed by removing one row of cylinders along (1,0) direction shown in Fig. 1b. The band structures with the filling fraction f=0.283 is shown in part B, Fig. 2. Comparing part B with part A in Fig. 2, it can be seen that no band gaps exist within 3.32 to 4.45 when the straight linear defect is introduced. There are many defect bands, named guiding modes, arising in the absolute band gap with a certain degree of slope. This means that this kind of linear defect can act as a straight waveguide for almost all the flexural waves with frequencies falling in the band gap.

The complete guiding of waves associated with certain frequencies marked with "×" in part B, Fig. 2 can be visualized by depicting the displacement distributions in Fig. 3. Noted that the displacements at or near the defects are much larger than those of other points, which indicates that the propagation is mainly

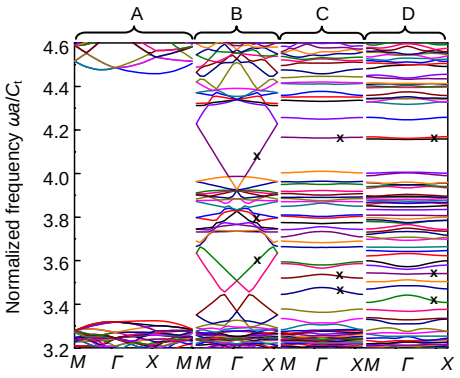

The complete guiding of waves associated with certain frequencies in part B, the flexural waves could propagate along the bending path at certain frequencies in part C, and the displacement distributions for frequencies at normal or flat bands in part D are marked with "×"

Fig. 2 Band structures of phononic crystals
(a) Perfect periods; (b) Straight linear defect; (c) Bending linear defect; (d) Branching linear defect

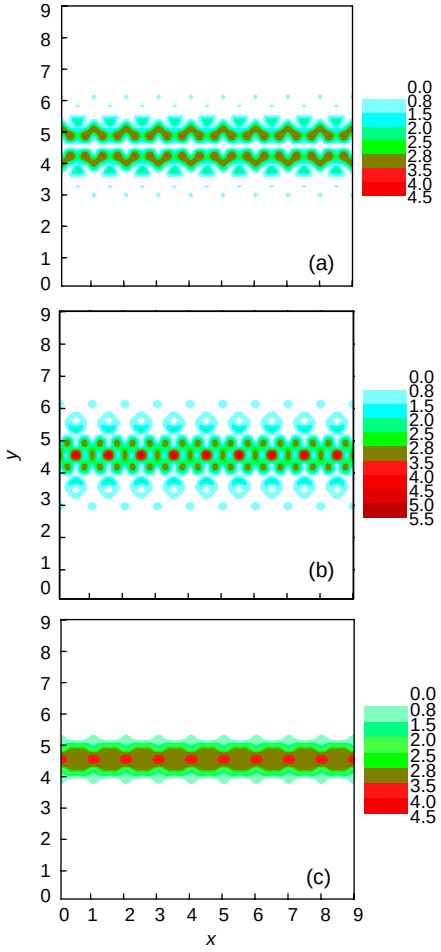

Fig. 3 Displacement distributions for the straight linear defect in the 9×9 supercell at the middle point of *ΓX* corresponding to the defect mode
(a) $\omega a/C_t$= 3.5985; (b) $\omega a/C_t$=3.7739; (c) $\omega a/C_t$=4.0763

confined to the straight channel. Further analysis shows that the larger the slope of the defect band, the better are the flexural waves guided. Similar behaviors have been observed in 2D infinite periodic systems (Li and Liu, 2005).

It is interesting to see from parts B–D in Fig. 2 that the defect bands are symmetric between *ΓX* and *ΓM* directions to a great extent, but the pass bands outside the band gap are not symmetric. It could be conjectured that the wave vector *ΓM* can be decomposed into *ΓX* and *XM*, and when the linear defects displayed in Fig. 1 are introduced, the waves in the *XM* direction are so localized that they can hardly propagate. Therefore, the wave propagation in the *ΓM* direction is almost the same as those in the *ΓX* direction for the defect modes.

3.2 Bending linear defect

Considering the bending linear defect, the dispersion curves are presented in part C, Fig. 2. We can see that there exist normal and flat defect bands separating the large band gap into several small ones. Most of the flat bands are located around the middle of the gap whilst normal bands are likely to appear at lower frequencies inside the gap. In general, the flat and normal bands correspond to the localized modes and guided modes, respectively. This can be demonstrated by the displacement distributions shown in Fig. 4. Figs. 4a and 4b show that the flexural waves could propagate along the bending path at certain frequencies marked with "×" in part C, Fig. 2, but obviously the guiding is not as efficient as that of the straight linear one. This may be understood by comparing the slopes of the dispersion curves in part C with those in part B, Fig. 2. Fig. 4c displays that the waves with frequencies in the flat bands are so localized that they cannot be transmitted through the bending path.

3.3 Branching linear defect

The dispersion curves for the phononic crystal thin plate with a branching linear defect are presented in part D, Fig. 2. Comparing part D with part C in Fig. 2, note that more defect bands appear in the band gap, and that normal bands are found mainly in the bottom of the gap which is similar to the case of the bending defect. In particular, several flat bands appear in the region where guided modes exist for the bending defect, indicating that some guided modes for the bending configuration are converted into the localized modes due to the introduction of the branching defect.

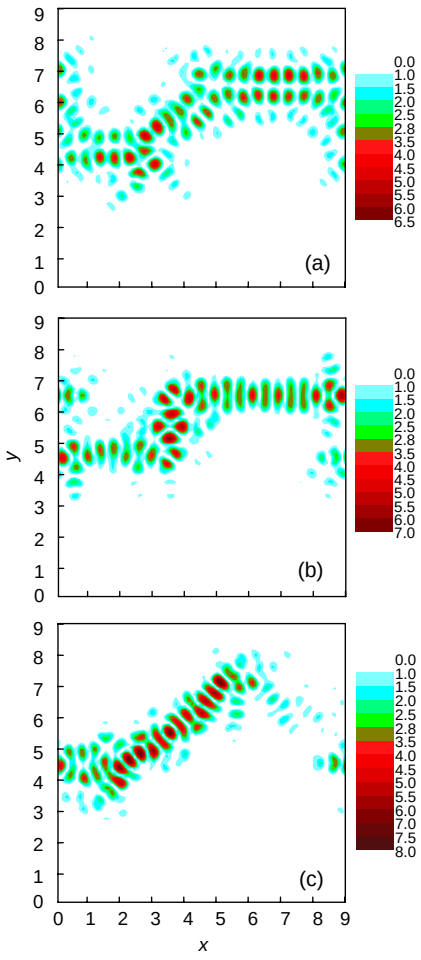

Fig. 4 Displacement distributions for the bending linear defect in the 9×9 supercell at the middle point of *ΓX* corresponding to the defect mode
(a) $\omega a/C_t$=3.4619; (b) $\omega a/C_t$=3.5268; (c) $\omega a/C_t$=4.165

The displacement distributions for frequencies at normal or flat bands marked with "×" in part D, Fig. 2 are also illustrated in Fig. 5 which shows that the displacement distributions at upper and lower branches are symmetrical about the central horizontal line because of their geometrical symmetry. The flexural waves could propagate along the branching defect in the normal defect modes whilst being localized at or near some part of the linear defect in the flat defect modes.

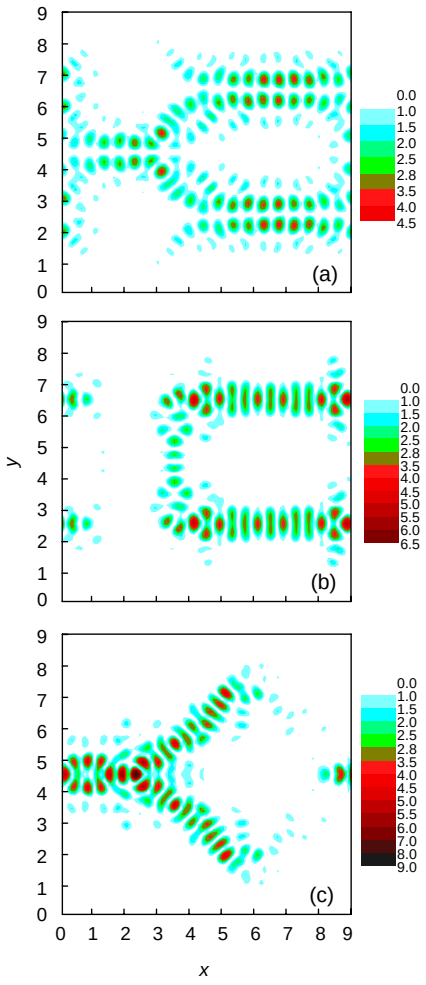

Fig. 5 Displacement distributions for the branching linear defect in the 9×9 supercell at the middle point of ΓX corresponding to the defect mode
(a) $\omega a/C_t$=3.4232; (b) $\omega a/C_t$=3.541; (c) $\omega a/C_t$=4.1584

4 Conclusions

Using the improved plane wave expansion method combined with the supercell technique, we investigated theoretically the properties of flexural waves propagating in phononic crystal thin plates with three kinds of configurations of linear defects. For the straight linear defect, the defect modes are all guiding modes and almost all the flexural waves with frequencies falling in the band gap of the perfect phononic crystals can propagate along the defect path. For the bending or branching linear defect, localized modes appear and the localization around the defects increases with the decreasing of the slopes of the defect bands. The defect modes arising at lower frequencies in the gap region tend to exhibit guiding properties. The results show that the defect modes are strongly dependent on the configurations of the linear defect. Straight linear defects can act as a high efficiency waveguide and the bending or branching defects could serve as waveguides or filters because of the existence of both guided and localized modes.

References

Benchabane, S., Khelif, A., Choujaa, A., Djafari-Rouhani, B., Laude, V., 2005. Interaction of waveguide and localized modes in a phononic crystal. *Europhysics Letters*, **71**(4): 570-575. [doi:10.1209/epl/i2005-10131-2]

Bria, D., Djafari-Rouhani, B., 2002. Omnidirectional elastic band gap in finite lamellar structures. *Physical Review E*, **66**(5):056609. [doi:10.1103/PhysRevE.66.056609]

Cao, Y.J., Hou, Z.L., Liu, Y.Y., 2004. Convergence problem of plane-wave expansion method for phononic crystals. *Physics Letters A*, **327**(2-3):247-253. [doi:10.1016/j.physleta.2004.05.030]

Charles, C., Bonello, B., Ganot, F., 2006. Propagation of guided elastic waves in 2D phononic crystals. *Ultrasonics*, **44**(Suppl. 1):e1209-e1213. [doi:10.1016/j.ultras.2006.05.096]

Hsu, J.C., Wu, T.T., 2006. Efficient formulation for band-structure calculations of two-dimensional phononic-crystal plates. *Physical Review B*, **74**(14):144303. [doi:10.1103/PhysRevB.74.144303]

Kafesaki, M., Sigalas, M.M., Garcia, N., 2001. Wave guides in two-dimensional elastic wave band-gap materials. *Physica B: Condensed Matter*, **296**(1-3):190-194. [doi:10.1016/S0921-4526(00)00799-7]

Khelif, A., Choujaa, A., Djafari-Rouhani, B., Wilm, M., Ballandras, S., Laude, V., 2003a. Trapping and guiding of acoustic waves by defect modes in a full-band-gap ultrasonic crystal. *Physical Review B*, **68**(21):214301. [doi:10.1103/PhysRevB.68.214301]

Khelif, A., Djafari-Rouhani, B., Vasseur, J.O., Deymier, P.A., 2003b. Transmission and dispersion relations of perfect and defect-containing waveguide structures in phononic band gap materials. *Physical Review B*, **68**(2):024302. [doi:10.1103/PhysRevB.68.024302]

Khelif, A., Choujaa, A., Benchabane, S., Djafari-Rouhani, B., Laude, V., 2004. Guiding and bending of acoustic waves in highly confined phononic crystal waveguides. *Applied Physics Letters*, **84**(22):4400-4402. [doi:10.1063/1.1757642]

Li, L.F., 1996. Use of Fourier series in the analysis of discontinuous periodic structures. *Journal of the Optical Society America A*, **13**(9):1870-1876. [doi:10.1364/JOSAA.13.001870]

Li, X.C., Liu, Z.Y., 2005. Bending and branching of acoustic waves in two-dimensional phononic crystals with linear defects. *Physics Letters A*, **338**(3-5):413-419. [doi:10.1016/j.physleta.2005.02.056]

Pennec, Y., Djafari-Rouhani, B., Vasseur, J.O., Khelif, A., Deymier, P.A., 2004. Tunable filtering and demultiplexing in phononic crystals with hollow cylinders. *Physical Review E*, **69**(4):046608. [doi:10.1103/PhysRevE.69.046608]

Pennec, Y., Djafari-Rouhani, B., Larabi, H., Vasseur, J.O., Hladky-Hennion, A.C., 2008. Low-frequency gaps in a phononic crystal constituted of cylindrical dots deposited on a thin homogeneous plate. *Physical Review B*, **78**(10):104105. [doi:10.1103/PhysRevB.78.104105]

Sigalas, M.M., 1998. Defect states of acoustic waves in a two-dimensional lattice of solid cylinders. *Journal of Applied Physics*, **84**(6):3026-3030. [doi:10.1063/1.368456]

Sigalas, M.M., Economou, E.N., 1994. Elastic waves in plates with periodically placed inclusions. *Journal of Applied Physics*, **75**(6):2845-2850. [doi:10.1063/1.356177]

Sun, J.H., Wu, T.T., 2005. Analyses of mode coupling in joined parallel phononic crystal waveguides. *Physical Review B*, **71**(17):174303. [doi:10.1103/PhysRevB.71.174303]

Sun, J.H., Wu, T.T., 2007. Propagation of acoustic waves in phononic-crystal plates and waveguides using a finite-difference time-domain method. *Physical Review B*, **76**(10):104304. [doi:10.1103/PhysRevB.76.104304]

Tanaka, Y., Tamura, S.I., 1998. Surface acoustic waves in two-dimensional periodic elastic structures. *Physical Review B*, **58**(12):7958-7965. [doi:10.1103/PhysRevB.58.7958]

Vasseur, J.O., Hladky-Hennion, A.C., Djafari-Rouhani, B., Duval, F., Dubus, B., Pennec, Y., Deymier, P.A., 2007. Waveguiding in two-dimensional piezoelectric phononic crystal plates. *Journal of Applied Physics*, **101**(11):114904. [doi:10.1063/1.2740352]

Vasseur, J.O., Deymier, P.A., Djafari-Rouhani, B., Pennec, Y., Hladky-Hennion, A.C., 2008. Absolute forbidden bands and waveguiding in two-dimensional phononic crystal plates. *Physical Review B*, **77**(8):085415. [doi:10.1103/PhysRevB.77.085415]

Wu, F.G., Liu, Z.Y., Liu, Y.Y., 2004. Splitting and tuning characteristics of the point defect modes in two-dimensional phononic crystals. *Physical Review E*, **69**(6):066609. [doi:10.1103/PhysRevE.69.066609]

Wu, T.T., Huang, Z.G., Lin, S., 2004. Surface and bulk acoustic waves in two-dimensional phononic crystal consisting of materials with general anisotropy. *Physical Review B*, **69**(9):094301. [doi:10.1103/PhysRevB.69.094301]

Yan, Z.Z., Wang, Y.S., 2006. Wavelet-based method for calculating elastic band gaps of two-dimensional phononic crystals. *Physical Review B*, **74**(22):224303. [doi:10.1103/PhysRevB.74.224303]

Yan, Z.Z., Wang, Y.S., Zhang, C.Z., 2008. Wavelet method for calculating the defect states of two-dimensional phononic crystals. *Acta Mechanica Solida Sinica*, **21**(2):104-109. [doi:10.1007/s10338-008-0813-6]

Yao, Y.W., Wu, F.G., Hou, Z.L., Liu, Y.Y., 2007. Propagation properties of elastic waves in semi-infinite phononic crystals and related waveguides. *The European Physical Journal B*, **58**(4):353-360. [doi:10.1140/epjb/e2007-00244-x]

Yao, Z.J., Yu, G.L., Wang, Y.S., Shi, Z.F., 2009. Propagation of bending waves in phononic crystal thin plates with a point defect. *International Journal of Solids and Structures*, **46**(13):2571-2576. [doi:10.1016/j.ijsolstr.2009.02.002]

Yu, D.L., Wang, G., Liu, Y.Z., Wen, J.H., Qiu, J., 2006. Flexural vibration band gaps in thin plates with two-dimensional binary locally resonant structures. *Chinese Physics*, **15**(2):266-271. [doi:10.1088/1009-1963/15/2/004]

Zhang, X., Liu, Z., Liu, Y., Wu, F., 2004. Defect states in 2D acoustic band-gap materials with bend-shaped linear defects. *Solid State Communications*, **130**(1-2):67-71. [doi:10.1016/j.ssc.2004.01.007]

Zhang, X., Wu, F., Yao, Y., Liu, Z., 2010. Transverse wave-band gaps and longitudinal wave band gaps in solid phononic crystals. *Solid State Communications*, **150**(5-6):275-279. [doi:10.1016/j.ssc.2009.11.007]

Zhong, H.L., Wu, F.G., Zhang, X., Liu, Y.Y., 2005. Localized defect modes of water waves through two-dimensional periodic bottoms with point defects. *Physics Letters A*, **339**(6):478-487. [doi:10.1016/j.physleta.2005.03.062]